Polym. Bull. (2017) 74:4423–4436
DOI 10.1007/s00289-017-1966-6

ORIGINAL PAPER

PBAT/organoclay composite films: preparation and properties

Gabriella A. M. Falcão[1] · Maria B. C. Vitorino[1] · Tatiara G. Almeida[1] · Marcelo A. G. Bardi[1] · Laura H. Carvalho[1] · Eduardo L. Canedo[1]

Received: 5 October 2016 / Revised: 23 January 2017 / Accepted: 28 February 2017 /
Published online: 3 March 2017

Abstract Environmental problems caused by the increased waste associated with short-term use of plastic materials, particularly by the food packaging industry, prompted the search for biodegradable alternatives. This contribution studied one of these alternatives, poly(butylene adipate-co-terephthalate)—PBAT, a polymer that is fully biodegradable in common landfills, compounded with a small amount of Cloisite 20A organoclay. Materials were mixed in a laboratory internal mixer and films prepared in a chill roll extruder. Results show that the presence of organoclay does not increase degradation of the polymer matrix during processing, nor affects its crystallization characteristics. However, organoclay addition significantly diminished oxygen and carbon dioxide permeability of the films, making them a very interesting alternative for the food packaging industry.

Keywords PBAT · Organoclay · Films

Introduction

The degradation of the natural environment by human action has been pushing the search for solutions compatible with social and economic growth. One of the main environmental problems created by contemporary civilization in industrial societies is the increase in plastic products such as food containers, films, foams, bottles, etc., discarded in landfills. There are no simple answers to this problem. Recycling of used parts is being explored as a possible solution, but recycling is a universal answer to the disposal of plastic waste. Another promising approach is the use of

✉ Eduardo L. Canedo
ecanedo2004@yahoo.com

[1] Department of Materials Engineering, Federal University of Campina Grande, Campina Grande, PB 58429-140, Brazil

biodegradable materials. Biodegradable plastics, that can be digested by aerobic microorganisms (bacteria and molds), which are normally present in soil, and returned to the atmosphere as carbon dioxide and water in a matter of months (not years or even centuries), are an interesting alternative [1, 2].

Poly(butylene adipate-*co*-terephthalate) (PBAT) is considered one of the most promising polymers for biodegradable films for the food packaging industry [3]. PBAT is a synthetic aliphatic–aromatic copolyester, which fully degrades within a few weeks with the aid of enzymes naturally present in fertile soil. The aliphatic moiety is responsible for its biodegradability, and the aromatic part provides good mechanical properties compared to other polymers [4]. PBAT is a flexible plastic, designed for film extrusion and extrusion coating, has high elongation at break, as well as a good processability. Its mechanical properties are similar to those of polyethylene films [5, 6]. It has been applied in the manufacture of agricultural films and laminated films for solid food packaging and garbage bags [7].

However, poor barrier properties limit its applications in industrial packaging. Thus, research efforts were focused on modifying PBAT permeability to gas and vapors; one such modification was the incorporation of nanoscale fillers [8–11].

Azeredo and Jimenez et al. [12, 13], studied nanocomposite films PBAT/clay and reported improvements of mechanical, thermal, and barrier properties without additional processing or cost increases, while complete biodegradability was retained [3, 14]. Bio-nanocomposite films of PBAT and blends, with a low layered silicate filler content, displaying improved mechanical properties and thermal stability have been developed in recent years [15–18].

This contribution is concerned with the processing of PBAT/organoclay nanocomposites with 1, 3 and 5% loadings by melt mixing in an internal mixer. Flat films about 100 mm thick were prepared by extrusion and characterized by X-ray diffraction, infrared spectroscopy and differential scanning calorimetry. The oxygen and carbon dioxide permeability of these films was determined as a function of organoclay content.

Experimental

The poly(butylene adipate-*co*-tephthalate) [PBAT] is a statistical copolymer with approximately an equal number of each structural unit as shown below

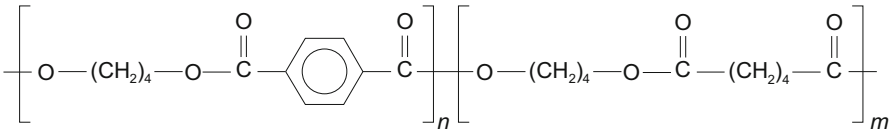

Supplied by BASF (Germany) under commercial name Ecoflex®, grade F-C1200, the polymer has a density of 1.26 g/cm^3 at room temperature, with a melt flow rate of 3–5 dg/min (ISO 1133, 190 °C/2.16 kg), glass transition temperature −30 °C, and melting point between 110 and 115 °C according to the manufacturer [5]. A

higher melting point, around 135 °C, was measured in our lab, along with a low degree of crystallinity, 10–15% [16].

The organoclay was Cloisite®20A purchased from Southern Clay Products (USA). It is a natural layered silicate (montmorillonite) with cation exchange capacity 0.95 meq/g, modified with quaternary ammonium salt with two long-chain (C16 to C18) aliphatic residues. According to the manufacturer it has a basal interplanar distance of 2.42 nm and a density of 1.72 g/cm^3. A granulometric analysis, performed with laser instrument Cilas 1064 LD, measured an average particle diameter of 8.2 μm, with 80% of the particles ranging in size from 1.7 to 15.7 μm.

Samples with 1, 3, and 5% organoclay content (by weight) were prepared in a Haake Rheomix 3000 laboratory internal mixer, fitted with high-intensity (roller type) rotors. The processing chamber wall was kept at a constant temperature of 160 °C and the fill factor was estimated at 75%. The mixer was operated at 60 rpm for 10 min. Samples of the neat PBAT matrix were also processed to provide a baseline for comparison.

The compounds produced in the mixer were ground and fed to a 16-mm bench scale single screw extruder Lab-16 Chill-Roll from AX Plásticos (Brazil) with a flat die, operating at 180 °C and 45 rpm, to prepare films for further characterization. Film thickness between 95 and 125 μm was measured for the different compounds; thickness uniformity for individual films was ±5 μm.

The organoclay and the PBAT/organoclay films were characterized by X-ray diffraction (XRD) using a Shimadzu XDR-6000 instrument, with incident radiation of $\lambda = 0.154$ nm wavelength; data were collected from 2° to 12° (2θ) at a scanning rate of 1°/min. Basal interplanar distances were computed using Bragg's law. Differential scanning calorimetry (DSC) tests were conducted in TA Instruments DSC Q20, with film samples of approximately 5 mg in an inert atmosphere, following a thermal program in three stages: heating from 25 to 200 °C, cooling to 25 °C and reheating to 200 °C, at a heating/cooling rate of 10 °C/min. The raw time/temperature heat-flow data were integrated using custom software and thermal parameters (temperatures and rates, crystallinity, etc.) computed for all phase-transition events detected. Permeability to oxygen and carbon dioxide gases was measured at 25 °C in a GPD-C Brugger instrument according to ASTM D1434 e ISO 15105/1 standards.

Results and discussion

X-ray diffraction

X-ray diffraction patterns for the organoclay (C20A), neat PBAT matrix, and the compounds are shown in Fig. 1.

They show a significant expansion of the clay upon incorporation into the polymer matrix, with the interplanar basal distance (separation between the clay layers) increasing from 2.6 nm to more than 3.8 nm. This suggests a fair degree of intercalation of the polymer chain in the clay structure, with qualifies the

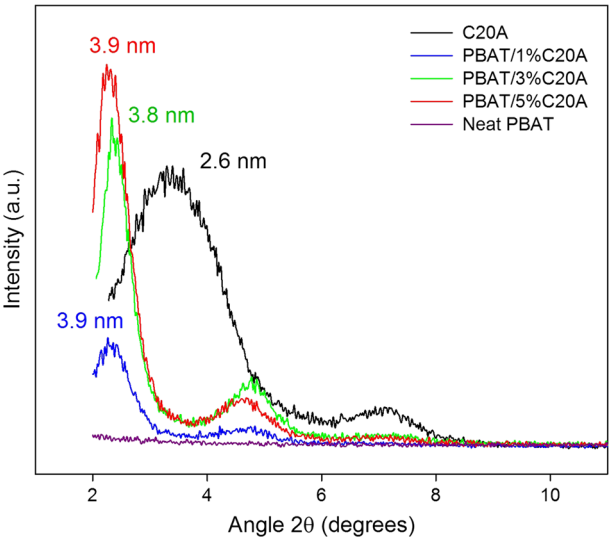

Fig. 1 X-ray diffraction patterns for the organoclay (C20A), the PBAT and the PBAT/C20A films

compounds as nanocomposites. However, no sign of exfoliation was detected in peak structure.

PBAT is a polar resin, which may interact favorably with the surface of the organoclay, even in the absence of a compatibilizer, through dipole–dipole and hydrogen bonding. The significant intercalation shown by XRD as an increase in the interlayer spacing of the clay suggests that. However, exfoliation depend more processing conditions (high shear stresses) than on structural factors [19]. The preparation methods employed in the present work (internal mixer, single screw extrusion) did not provide the high stresses needed for significant exfoliation, reflected in the relatively sharp XDR peaks [20].

Torque rheometry

Temperature inside the processing chamber (T) and total torque (Z) were measured as a function of time (t) during compounding in the internal mixer. Results are presented in Fig. 2.

The plots suggest that after 4 min the matrix is substantially molten. We may assume that torque changes due to increasing degree of dispersion (if any) are negligible during the terminal stage of melt processing, identified here as the last 2 min inside chamber (8–10 min processing time). Since at constant rotor speed torque is directly proportional to melt viscosity at this stage, decrease of torque with time may be attributed to increases in melt temperature and decreases in molar mass of the polymer due to degradation during processing [21].

Temperature effects on the viscosity (that is, on torque) may be eliminated by adjusting the torque to a constant reference temperature (T^*):

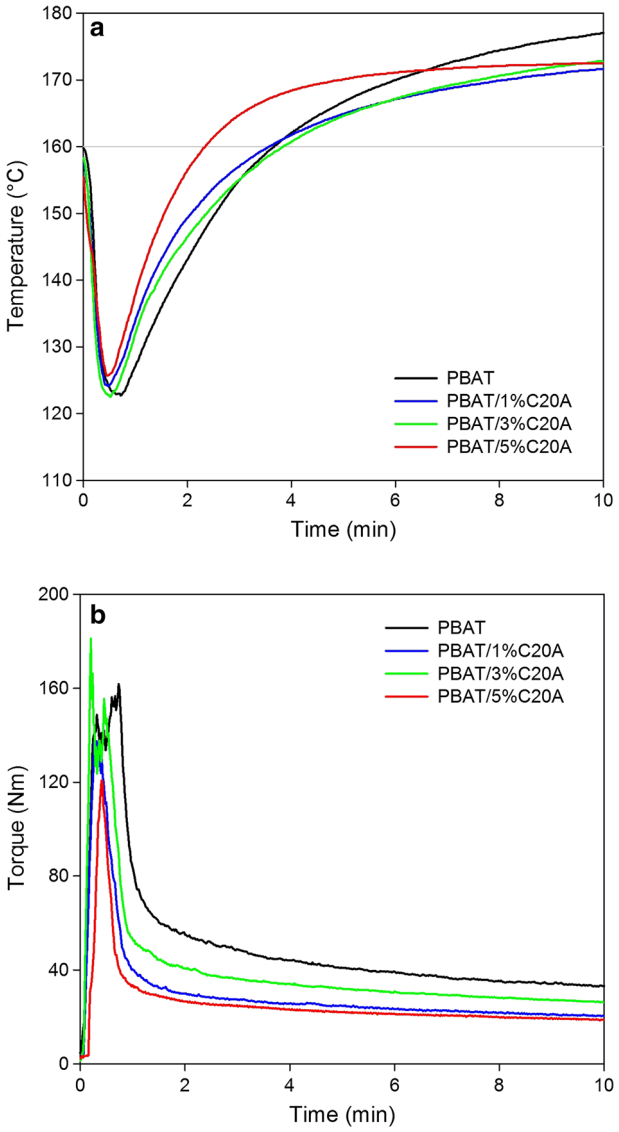

Fig. 2 Temperature (**a**) and torque (**b**) as function of time in the internal mixer chamber

$$Z^* = Z\exp\{\beta(T - T^*)\}, \tag{1}$$

where Z^* is the adjusted torque and β is the exponential temperature coefficient of the viscosity, taken here as 0.012 $°C^{-1}$ [22] Fig. 3 shows the evolution of Z^* during the last 2 min of processing.

Decrease in adjusted torque with time during this stage suggests incipient thermal degradation of the polymer matrix during processing. A relative rate of change of the adjusted torque is then a measure of the rate of degradation [23]:

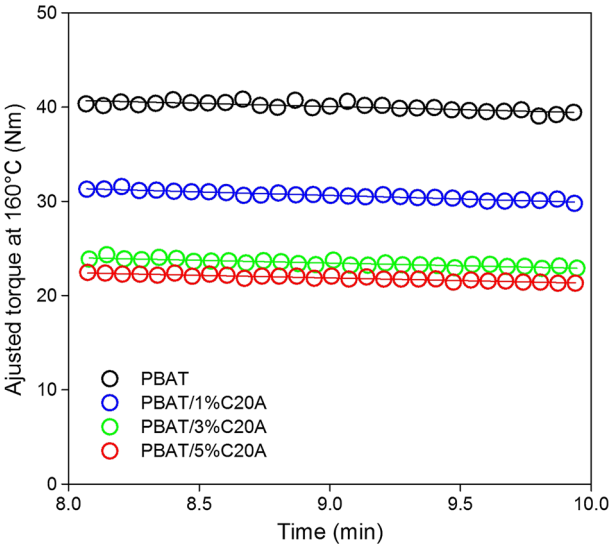

Fig. 3 Adjusted torque as function of time during the terminal stage of processing in the internal mixer

$$R_Z = -\frac{1}{\overline{Z^*}}\frac{\mathrm{d}Z^*}{\mathrm{d}t}. \tag{2}$$

Table 1 shows several parameters of interest for the melt processing of the neat PBAT matrix and the PBAT/C20A compounds.

The rate of change of molar mass may be estimated if the relation between viscosity and molar at processing conditions is known [21, 22]. For the PBAT processed in the laboratory, internal mixer/operating conditions used here [23]:

$$R_M \approx -\frac{1}{\Delta t}\left(\frac{\Delta Z^*}{\overline{Z^*}}\right)^{1/3}, \tag{3}$$

where R_M is the relative rate of change of the weight-average molar mass of the polymer. Nevertheless, R_Z is a useful rate constant, assuming a first order process; if expressed in min^{-1} $100 \times R_Z$ is the % change in torque for each minute of processing.

In the present case, a slight increase of the rate of degradation is observed (Table 1) as the clay content increases from 0% (neat matrix) to 5% C20A.

Table 1 Torque rheometry parameters during the terminal stage

Sample	$\bar{T}$ (°C)	$\overline{Z*}$ (Nm)	dZ*/dt	R_z (min^{-1})
PBAT	175.9	40.2	−0.699	0.0174
PBAT 1%	170.9	30.7	−0.735	0.0239
PBAT 3%	171.9	23.4	−0.540	0.0231
PBAT 5%	172.3	21.9	−0.558	0.0255

However, the rates are low and degradation under processing may be disregarded in first approximation.

Thermal properties

Figure 4 shows the raw data from the DSC, heat flow versus time, run with three-stage temperature program (at 10 °C/min heating/cooling rate) as described in the Experimental section, for the films of near PBAT and the PBAT/organoclay compounds.

Thee phase-transition events may be identified: melting of the crystalline fraction of the polymer during the first heating stage, crystallization from the melt during the cooling stage, and melting during the second heating stage.

For the melt crystallization event, the starting and end points of departure from the underlying baseline were visually established in a plot of heat flow (J) versus time (t). The fractional crystallization (or relative crystallinity) $x = x(t)$ for the event was computed by integration:

$$x(t) = \frac{1}{E_0}\int_{t_1}^{t} |J(t') - J_0(t')|\mathrm{d}t', \tag{4}$$

where J_0 is a suitable virtual baseline during the event and E_0 is the total latent heat of phase change:

$$E_0 = \int_{t_1}^{t_2} |J(t) - J_0(t)|\mathrm{d}t, \tag{5}$$

where t_1 and t_2 are the initial and final times. The rate of the phase change $c = c(t)$ is:

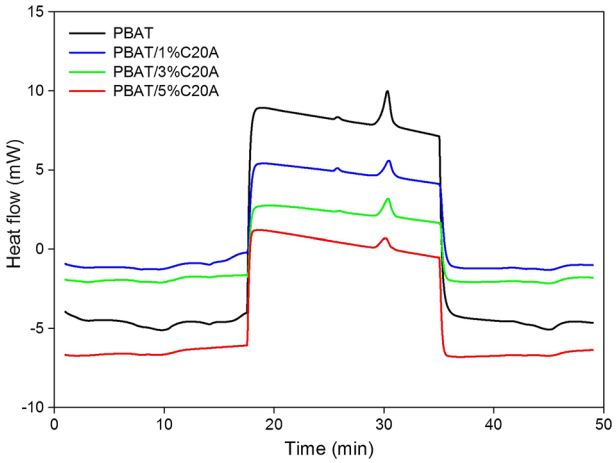

Fig. 4 Heat flow measured in the DSC as function of time for the net matrix (PBAT) and the PBAT/C20A nanocompounds

$$c(t) = \frac{\mathrm{d}x}{\mathrm{d}t} = \frac{|J(t) - J_0(t)|}{E_0}. \quad (6)$$

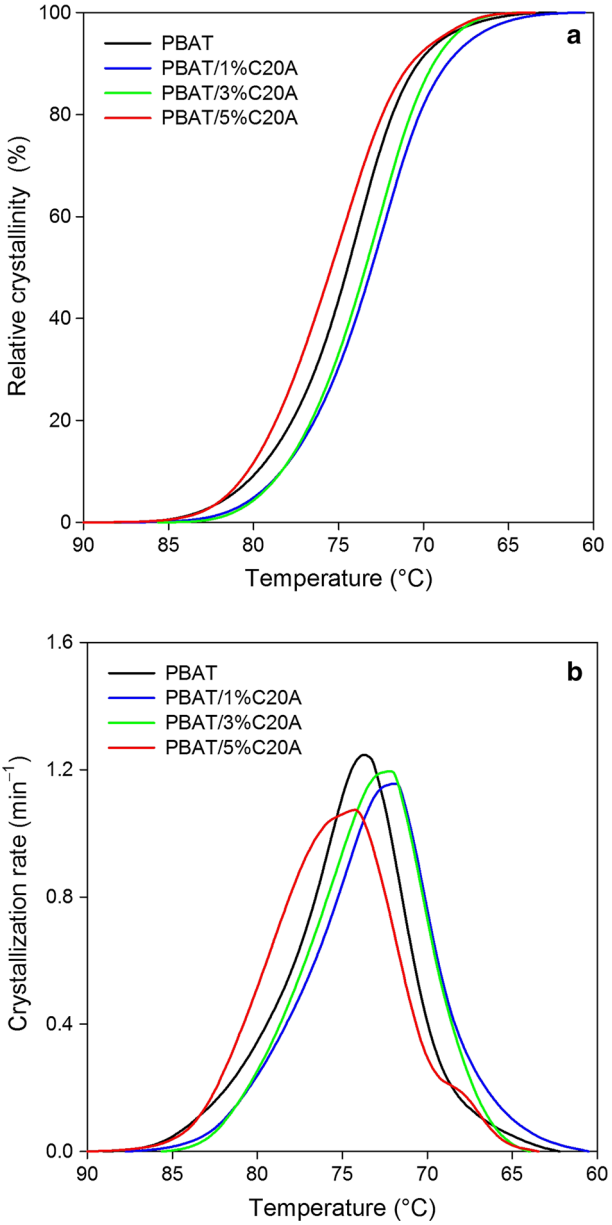

Fig. 5 Relative crystallinity (**a**) and crystallization rate (**b**) as function of temperature for the melt crystallization of PBAT and PBAT/organoclay nanocompounds

The fractional crystallization may be expressed as function of temperature (T), knowing the linear relationship between time and temperature during the event: $T = T_1 + \phi\,(t–t_1)$, where T_1 is the sample temperature at the starting point t_1 and $\phi = -\mathrm{d}T/\mathrm{d}t$ is the (constant) rate of cooling during the event.

The latent heat of phase change per unit of mass of crystallizable polymer (PBAT) is:

$$\Delta H = \frac{E_0}{m_S w_P}, \tag{7}$$

where, m_S is the sample mass and w_P is the mass fraction of PBAT in the sample. The mass crystallinty developed during the event is then estimated as:

$$\Delta X_c = \frac{\Delta H}{\Delta H_m^\circ}. \tag{8}$$

where, ΔH_m° is the specific enthalpy of crystallization of 100% crystalline material taken as $\Delta H_m^\circ = 114$ J/g for the PBAT [24].

Figure 5 shows the relative crystallinity and the crystallization rate as functions of temperature.

Table 2 shows some typical parameters of the crystallization process, including the crystallization temperature range (between 0.1 and 99.0% relative crystallinity), the crystallization peak temperature T_{cp}, the maximum crystallization rate $c_{\max}$, the crystallization half-time $\tau_{1/2}$, the latent heat of crystallization and the crystallinity.

Melt crystallization temperature was not affected by the presence and concentration of organoclay. Crystallization rate and crystallinity show moderate decreases: about 14% in maximum crystallization rate and 12% in crystallinity, comparing the PBAT/5% organoclay compound with the neat matrix. PBAT is a random copolymer. Results suggest that the presence of clay particles has slightly disturbed the already difficult crystal formation, and, in the absence of significant delamination of the layered silicate, this effect masked the possible increase in nucleating rate normally expected in filled melts. The crowding effect reported in other polyesters may have also affected crystal growth [25]. This is a very positive result for the intended application of the compounds as transparent packaging films.

The same procedure was applied to melting during the second heating stage. Conversion (molten fraction) x and melting rate c are plotted against temperature in Fig. 6, and typical parameters of the melting event for all composition tested are listed in Table 3.

Table 2 Parameters for the melt crystallization (C1) event

Sample	$T_{0.1}$–$T_{99.9\%}$ (°C)	T_{cp} (°C)	$c_{\max}$ (min^{-1})	$\tau_{1/2}$ (min)	ΔH_c (J/g)	ΔX_c (%)
PBAT	86.7–63.5	73.6	1.25	1.24	18.1	16.0
PBAT/1% C20A	85.4–62.0	72.0	1.16	1.24	17.0	15.0
PBAT/3% C20A	84.0–65.0	72.2	1.20	1.06	17.7	15.6
PBAT/5% C20A	87.1–65.0	74.2	1.07	1.17	16.1	14.1

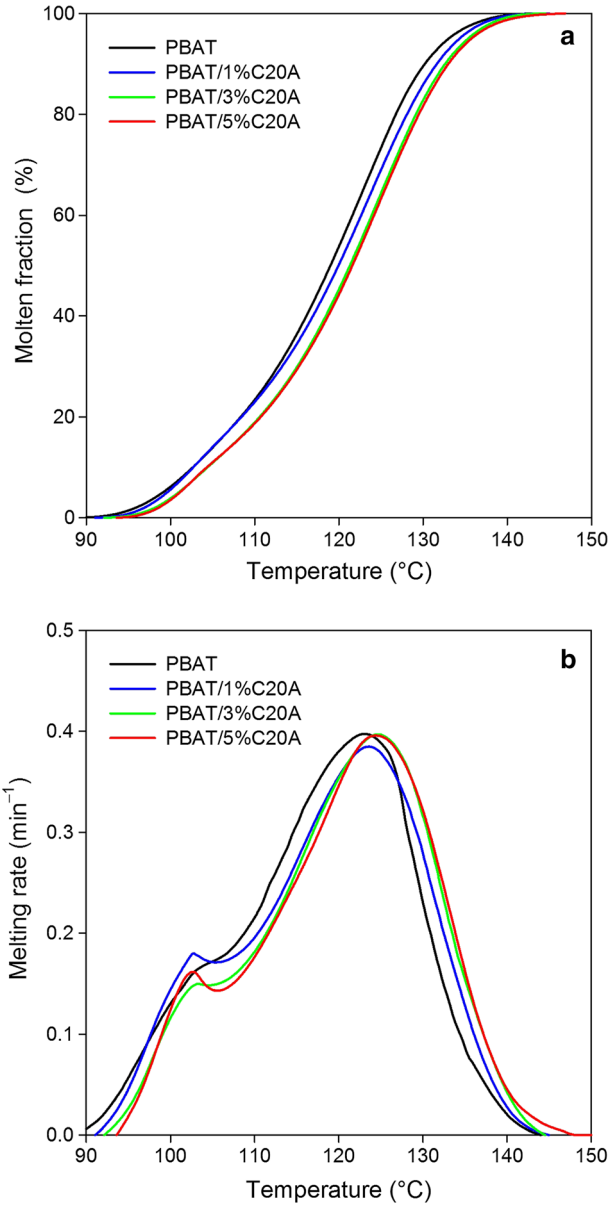

Fig. 6 Molten fraction (**a**) and melting rate (**b**) as function of temperature during the reheating stage for PBAT and PBAT/organocaly nanocompounds

Melting of the polymer matrix is shown as complex peak, with a minor component melting at about 20 °C lower temperature than the major event. An increase of 2 °C in the melting peak temperature and 3 °C in the final melting point were observed for PBAT/5% C20A compound, compared with the neat matrix

Table 3 Parameters for the second melting (F2) event

Sample	$T_{0.1}$–$T_{99.9\%}$ (°C)	T_{mp} (°C)	c_{max} (min^{-1})	ΔH_m (J/g)	ΔX_m (%)
PBAT	90.6–141.5	123.0	0.397	13.2	11.5
PBAT/1% C20A	92.6–142.2	123.6	0.385	12.0	10.5
PBAT/3% C20A	93.7–142.6	124.7	0.397	12.9	11.3
PBAT/5% C20A	95.0–145.1	125.0	0.396	12.6	11.1

Table 4 Permeability to oxygen and carbon dioxide

Sample	Permeability (10^{-6} cm^3 STP/cm-h-bar)	
	O_2	CO_2
PBAT	32.2 ± 1.8	372 ± 13
PBAT/1% C20A	30.9 ± 4.7	159 ± 26
PBAT/3% C20A	23.9 ± 2.3	145 ± 26
PBAT/5% C20A	14.2 ± 0.4	125 ± 8

PBAT, but melting rate and crystallinity were not affected. Again, the phase transition is remarkably independent of the presence of organoclay.

Permeability

Permeability to oxygen and carbon dioxide gases measured at 25 °C for the neat PBAT and PBAT/organoclay films with 1, 3 and 5% C20A is shown in Table 4 and plotted in Fig. 7. The presence and concentration of inert fillers usually lowers the permeability of films. In present case, the effect the organoclay was very significant: the incorporation 5% C20A in the PBAT matrix resulted in a 13% drop of oxygen permeability, and a drop of 24% in carbon dioxide permeability compared to the neat matrix value. Addition of organoclay lowers permeability to values comparable to premium packaging films (HDPE, LLDPE), which are much lower than ordinary LDPE film [26].

Films for food packaging applications require, in addition to low crystallinity and low oxygen and carbon dioxide permeability, reasonable mechanical properties. PBAT is well known for its excellent properties (high flexibility, impact and tearing resistance) [1, 2, 5, 6]. Organoclay nanocomposites are reported to improve and preserve these characteristics [9–17]. The enhanced mechanical properties and biodegradability of Ecoflex/Cloisite 20A films will be presented in a forthcoming publication.

Conclusions

Our data indicate that the addition of small amounts of organoclay (C20A) to PBAT does not increase degradation of the polymer matrix during processing, nor does it affect the crystallization process. These characteristics make nanocompounds of

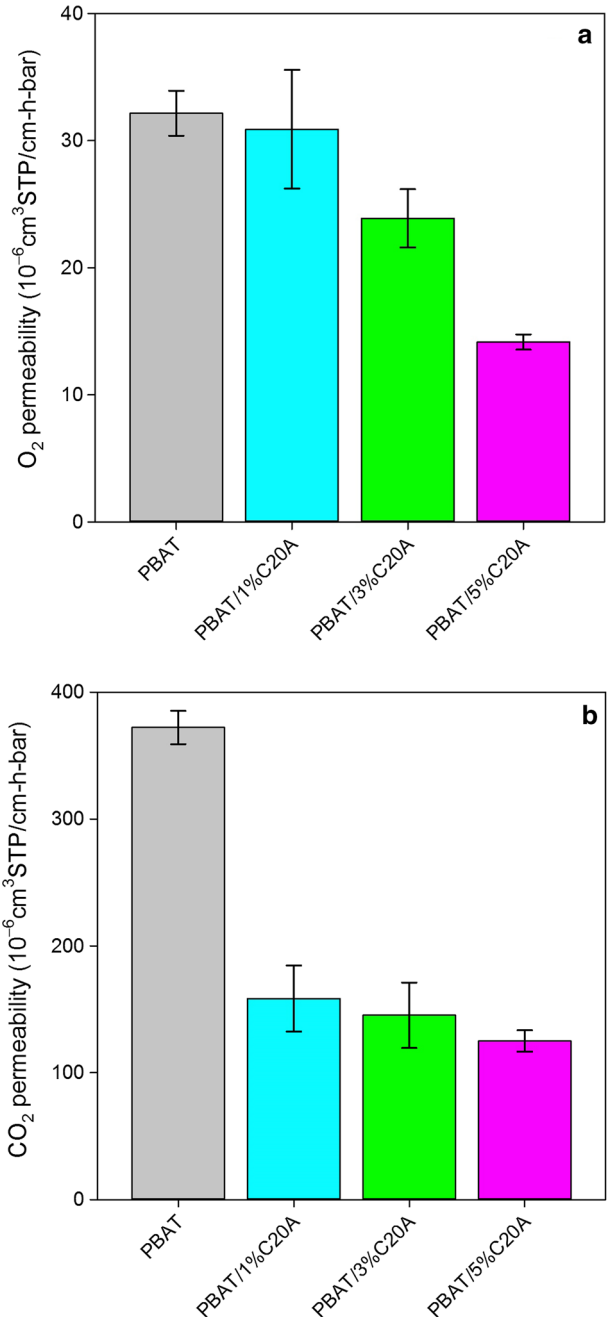

Fig. 7 Permeability to oxygen (**a**) and carbon dioxide (**b**) at ambient temperature for PBAT and PBAT/organoclay nanocompound films

PBAT with up to 5% organoclay suitable for the preparation of films for packaging industry, an interesting alternative to conventional materials, since the matrix is fully biodegradable in common landfills. The low permeability of the PBAT/C20A films to oxygen and carbon dioxide gases recommends these materials for food packing, where this property is a major concern. We have found that PBAT/C20A films appear to be good materials for this application: fully biodegradable with low permeability and processable by conventional methods.

Acknowledgements The authors thank BASF Brasil for supplying Ecoflex polymer, and to the *Conselho Nacional de Pesquisa* (CNPq) e *Coordenação de Aperfeiçoamento de Pessoal Superior* (CAPES), Grant # 473622/2013-0, for financial support.

References

1. Ebnesajjad S (ed) (2013) Handbook of biopolymers and biodegradable plastics. properties, processing, and applications. Elsevier, Amsterdam
2. Bastioli C (ed) (2014) Handbook of biodegradable polymers, 2nd edn. Smithers Rapra Technology, Shawbury
3. Mondal D, Bhowmick B, Maity D, Mollick MR, Rana D, Rangarajan V, Sen R, Chattopadhyay D (2015) Investigation on sodium benzoate release from poly(butylene adipate-co-terephthalate)/organoclay/sodium benzoate based nanocomposite film and their antimicrobial activity. J Food Sci 80:E602–E609
4. Bastarrachea L, Dhawan S, Sablani SS, Mah J-H, Kang D-H, Zhang J, Tang J (2010) Biodegradable Poly(butylene adipate-co-terephthalate) films incorporated with nisin: characterization and effectiveness against Listeria innocua. J Food Sci 75:E215–E224
5. Yamamoto M, Witt U, Skupin G, Beimborn D, Müller RJ (2002) Biodegradable aliphatic-aromatic polyesters: Ecoflex. In: Steinbüchel YDA (ed) Biopolymers-polyesters iii—applications and commercial products. Wiley, New York, p 299ss
6. Siegenthaler KO, Künkel A, Skupin G, Yamamoto M (2012) Ecoflex and Ecovio: biodegradable, performance-enabling plastics. Adv Polym Sci 241:91–136
7. Jiang L, Wolcott MP, Zhang J (2006) Study of biodegradable polylactide/poly(butylene adipate-co-terephthalate) blends. Biomacromolecules 7:199–207
8. Zini E, Scandola M (2011) Green composites: an overview. Polym Compos 32:1905–1915
9. Chieng BW, Ibrahim NA, Wan Yunus WMZ (2010) Effect of organo-modified montmorillonite on poly(butylene succinate)/poly(butylene adipate-co-terephthalate) nanocomposites. Express Polym Lett 4:4004–4414
10. Lin S, Guo W, Chen C, Ma J, Wang B (2012) Mechanical properties and morphology of biodegradable poly(lactic acid)/poly(butylene adipate-co-terephthalate) blends compatibilized by transesterification. Mater Des 36:604–608
11. Raja V, Natesan R, Thiyagu T (2015) Preparation and mechanical properties of poly(butylene adipate-co-terephthalate) polyvinyl alcohol/SiO2 nanocomposite films for packaging applications. J Polym Mater 32:93–101
12. Azeredo HMC (2009) Nanocomposites for food packaging applications. Food Res Int 42:1240–1253
13. Jiménez A, Arab-Therany E, González LS (2014) Progress in biodegradable packaging materials. In: Rhim JW (ed) Progress in nanomaterials for food packaging. Future Science/Mokpo National University, Mokpo, pp 51–65
14. Pollet E, Avérous L (2012) Clay nano-biocomposites based on PBAT aromatic copolyesters. In: Pollet E, Avérous L (eds) Environmental silicate nano-biocomposites. Springer, London, pp 219–235
15. Chen J-H, Chen C-C, Yang M-C (2011) Characterization of nanocomposites of poly(butylene adipate-co-terephthalate) blending with organoclay. J Polym Res 18:2151–2159
16. Yang F, Qiu Z (2011) Preparation, crystallization, and properties of biodegradable poly (butylene adipate-co-terephthalate)/organomodified montmorillonite nano-composites. J Appl Polym Sci 119:1426–1434

17. Fukushima K, Wu M-H, Bocchini S, Rasyida A, Yang M-C (2012) PBAT based nanocomposites for medical and industrial applications. Mater Sci Eng C 32:1331–1351
18. Livi S, Sar G, Bugatt V, Espuche E, Duchet-Rumeau J (2014) Synthesis and physical properties of new layered silicates based on ionic liquids: improvement of thermal stability, mechanical behaviour and water permeability of PBAT nanocomposites. RSC Adv 4:26452–26461
19. Utracki LA (2004) Clay-containing polymeric nanocomposites. Rapra Technology, Sawbury
20. Bhattacharya SN, Gupta RK, Kamal MR (2008) Polymeric nano-composites. Hanser, Munich
21. Alves TS, Neto JES, Silva SML, Carvalho LH, Canedo EL (2016) Process simulation of laboratory internal mixers. Polym Test 50:94–100
22. Costa ARM, Almeida TG, Silva SML, Carvalho LH, Canedo EL (2015) Chain extension in poly(-butylene adipate-co-terephthalate). Inline analysis in a laboratory internal mixer. Polym Test 42:115–121
23. Almeida TG, Neto JES, Costa ARM, da Silva AS, Carvalho LH, Canedo EL (2016) Degradation during processing in poly(butylene adipate-co-terephthalate)/vegetable fiber compounds estimated by torque rheometry. Polym Test 55:204–211
24. Mondal D, Bhowmick B, Mollick M, Masud R, Maity D, Ranjan Saha N, Chattopadhyay D (2014) Antimicrobial activity and biodegradation behavior of poly(butylene adipate-co-terephthalate)/clay nanocomposites. J Appl Polym Sci 131:40079–40088
25. Wang Y, Li L, Wang X, Teng C, Li L, Xue G, Gu X, Bian Z (2012) Crowding-induced crystallization of poly(ethylene terephthalate). J Macromol Sci Phys 51:1893–1903
26. Van Krevelen DW, Te Nijenhuis K (2009) Properties of polymers, 4th edn. Elsevier, Amsterdam